Supplementary Material

Supported ionic liquids as customizable materials to purify immunoglobulin G

Emanuel V. Capela[a], Jéssica Bairos[a], Augusto Q. Pedro[a], Márcia C. Neves[a], M. Raquel Aires-Barros[b], Ana M. Azevedo[b], João A.P. Coutinho[a,*], Ana P.M. Tavares, Mara G. Freire[a,*]

[a]CICECO – Aveiro Institute of Materials, Department of Chemistry, University of Aveiro, 3810-193 Aveiro, Portugal.

[b]IBB – Institute for Bioengineering and Biosciences, Department of Bioengineering, Instituto Superior Técnico, Universidade de Lisboa, Av. Rovisco Pais, 1049-001 Lisbon, Portugal.

* Corresponding authors

maragfreire@ua.pt

jcoutinho@ua.pt

Materials and Methods

Production of the mAbs

The CHO cell culture supernatant containing anti-human interleukin-8 (anti-IL-8) monoclonal antibodies were produced in-house by a CHO DP-12 clone#1934 (ATCC CRL-12445) using DHFR minus/methotrexate selection system, obtained from the American Type Culture Collection (LGC Standards, Middlesex, UK). CHO DP-12 cells were grown in a mixture of 75 % (v/v) of serum-free media formulated with 0.1 % Pluronic® F-68 and without L-glutamine, phenol red, hypoxanthine, or thymidine (ProCHO™5, Lonza Group Ltd, Belgium), and 25 % (v/v) of Dulbecco's modified Eagle's medium (DMEM), supplemented with 10 % (v/v) of ultra-low IgG fetal bovine serum (FBS). ProCHO™5 formulation contains 4 mmol·L^{-1} L-glutamine (Gibco®, Carlsbad, CA), 2.1 g·L^{-1} $NaHCO_3$ (Sigma–Aldrich), 10 mg·L^{-1} recombinant human insulin (Lonza), 0.07 % (v/v) lipids (Lonza), 1 % (v/v) antibiotics (100 U·mL^{-1} penicillin and 100 μg·mL^{-1} streptomycin) (Gibco®) and 200 nmol·L^{-1} methotrexate (Sigma). DMEM was formulated to contain 4 mmol·L^{-1} of L-glutamine, 4.5 g·L^{-1} of D-glucose, 1 mmol·L^{-1} of sodium pyruvate, 1.5 g·L^{-1} of $NaHCO_3$, 2 mg·L^{-1} of recombinant human insulin, 35 mg·L^{-1} of L-proline (all acquired at Sigma), 0.1 % (v/v) of a trace element A, 0.1 % (v/v) of a trace element B (both from Cellgro®, Manassas, VA, USA), and 1 % (v/v) of antibiotics (100 U·mL^{-1} of penicillin and 100 μg·mL^{-1} of streptomycin from Gibco®). The composition of trace element A includes 1.60 mg·L^{-1} of $CuSO_4 \cdot 5H_2O$, 863.00 mg·L^{-1} of $ZnSO_4 \cdot 7H_2O$, 17.30 mg·L^{-1} of selenite·2Na, and 1155.10 mg·L^{-1} of ferric citrate, while the trace element B is composed of 0.17 mg·L^{-1} of $MnSO_4 \cdot H_2O$, 140.00 mg·L^{-1} of $Na_2SiO_3 \cdot 9H_2O$, 1.24 mg·L^{-1} of molybdic acid, ammonium salt, 0.65 mg·L^{-1} of NH_4VO_3, 0.13 mg·L^{-1} of $NiSO_4 \cdot 6H_2O$, and 0.12 mg·L^{-1} of $SnCl_2$. Cultures were carried out in T-75 flasks (BD Falcon, Franklin Lakes, NJ) at 37 (±1) °C and 5 % CO_2 with an initial cell density of 2.1×10^6 cells·mL^{-1}. Cell passages were performed every 4 days in a laminar flow chamber. Cell supernatants were centrifuged in BD Falcon™ tubes at 175 × g for 7 min, collected and stored at -20 °C. This culture was maintained for several months, with the mAbs concentration varying between 40.5 and 99.4 mg·L^{-1}.

Bonding amount

Equations to calculate the bonding amount in the different materials

The chemical amount of IL per area of material, designated by bonding amount (BA) (µmol m^{-2}), was determined for [Si][C_3]Cl and for the synthetized SILs. Considering the S_{BET} of silica 435 m^2/g, the BA value were calculated according with Eqs. (S1-S3)

For [Si][C_3]Cl, the amount of carbon was considered and Eq. (S1) was employed, where % C is the weight percentage of carbon, M(C) is the molar mass of carbon (g/µmol) and S_{BET} is the specific surface area of the initial silica:

$$\mathrm{BA} = \frac{\frac{\%\mathrm{C}}{3\times\mathrm{M(C)}}}{\mathrm{S_{BET}}} \tag{S1}$$

The BA of immidazollium based SIL, [Si][C_3mim]Cl, was calculated taking into account the amount of nitrogen present and that the immidazol ring contains two nitrogens atoms, according to Eq. (S2):

$$\mathrm{BA} = \frac{\frac{\%\mathrm{N}}{2\times\mathrm{M(N)}}}{\mathrm{S_{BET}}} \tag{S2}$$

For the ammonium based SILs Eq. (S3) was used to determine the BA, considering that only one nitrogen atom is present for each IL moiety. In the last cases (Eq. S1 and S2) %N is the weight percentage of nitrogen, M(N) is the molar mass of nitrogen (g/µmol), and S_{BET} is the specific surface area of the initial silica (435 m^2/g).

$$\mathrm{BA} = \frac{\frac{\%\mathrm{N}}{\mathrm{M(N)}}}{\mathrm{S_{BET}}} \tag{S3}$$

Determination of the SIL-based process performance

IgG calibration curve

The calibration curve of IgG was established with commercial human IgG, for 8 different concentrations: 5, 10, 15, 20, 50, 100, 150 and 200 mg·L^{-1}.

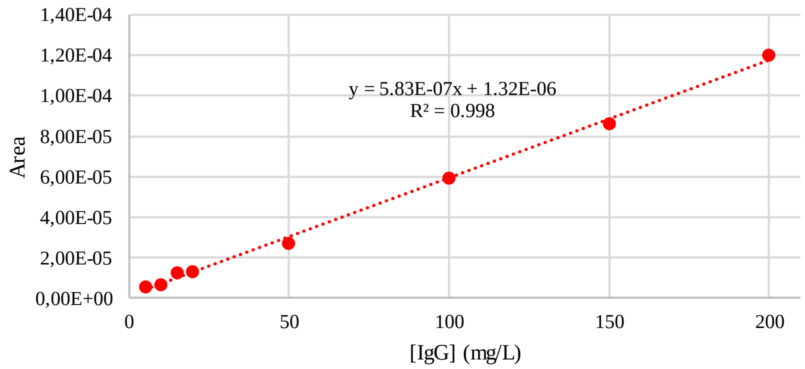

Fig. S1. Immunoglobulin G calibration curve established by SE-HPLC within the range 5, 10, 15, 20, 50, 100, 150 and 200 mg.L^{-1}.

Equations used to calculate the recovery yield (%Yield$_{IgG}$) of IgG, the percentage purity level of IgG (%Purity$_{IgG}$) and the aggregation percentage of IgG (%Aggregation$_{IgG}$) retained in the solution and in the material

The recovery yield (%Yield$_{IgG}$) of IgG retained in solution was determined according to the Eq. (S4):

$$\%\mathrm{Yield}_{\mathrm{IgG}} = \frac{[\mathrm{IgG}]_{\mathrm{final}} \times \mathrm{V}_{\mathrm{final}}}{[\mathrm{IgG}]_{\mathrm{initial}} \times \mathrm{V}_{\mathrm{initial}}} \times 100 \qquad \text{(S4)}$$

where $[IgG]_{initial}$ and $[IgG]_{final}$ correspond to the concentration of IgG in the initial complex media (before being in contact with the material) and of aqueous solutions after contact with the material, respectively. $V_{initial}$ and V_{final} corresponds to initial and final volumes, which is the same for both cases, 0.5 mL.

The percentage purity level of IgG was determined according to the Eq. (S5):

$$\%\mathrm{Purity}_{\mathrm{IgG}} = \frac{\mathrm{A}_{\mathrm{IgG}}}{\mathrm{A}_{\mathrm{Total}}} \times 100 \tag{S5}$$

where A_{IgG} corresponds to the SE-HPLC peak area of IgG and A_{Total} corresponds to the total area of the peaks corresponding to all proteins present in the respective sample.

The aggregation percentage of IgG was determined according to the Eq. (S6):

$$\%\mathrm{Aggregation}_{\mathrm{IgG}} = \frac{\mathrm{A}_{\mathrm{IgG\ aggregates}}}{\mathrm{A}_{\mathrm{IgG}}} \times 100 \tag{S6}$$

where $A_{IgG\ aggregates}$ corresponds to the SE-HPLC peak area of IgG aggregates.

In the cases where IgG was adsorbed on the supported materials, the $\%Yield_{IgG}$ in the material was determined according to the Eq. (S7):

$$\%\ \mathrm{Yield}_{\mathrm{IgG}} = \frac{([\mathrm{IgG}]_{\mathrm{initial}} \times \mathrm{V}_{\mathrm{initial}}) - ([\mathrm{IgG}]_{\mathrm{final}} \times \mathrm{V}_{\mathrm{final}})}{[\mathrm{IgG}]_{\mathrm{initial}} \times \mathrm{V}_{\mathrm{initial}}} \times 100 \tag{S7}$$

while the purity level of IgG being determined according to the Eq. (S8):

$$\%\ \mathrm{Purity}_{\mathrm{IgG}} = \frac{\mathrm{A}_{\mathrm{initial\ IgG}} - \mathrm{A}_{\mathrm{final\ IgG}}}{(\mathrm{A}_{\mathrm{initial\ IgG}} - \mathrm{A}_{\mathrm{final\ IgG}}) + (\mathrm{A}_{\mathrm{initial\ imp.}} - \mathrm{A}_{\mathrm{final\ imp.}})} \times 100 \tag{S8}$$

where the $A_{initial\ IgG}$ and $A_{final\ IgG}$ correspond to the SE-HPLC peak area of IgG of the initial complex media (before being in contact with the material) and aqueous solutions (after contact with the material), respectively. $A_{initial\ imp.}$ and $A_{final\ imp.}$ represent the SE-HPLC area of the peak of protein impurities in the initial complex media (before being in contact with the material), respectively.

In these cases, the aggregation percentage of IgG was determined according to the Eq. (S9):

$$\%\ \mathrm{Aggregation}_{\mathrm{IgG}} = \frac{\mathrm{A}_{\mathrm{initial\ aggregates}} - \mathrm{A}_{\mathrm{final\ aggregates}}}{(\mathrm{A}_{\mathrm{initial\ aggregates}} - \mathrm{A}_{\mathrm{final\ aggregates}}) + (\mathrm{A}_{\mathrm{initial\ IgG}} - \mathrm{A}_{\mathrm{final\ IgG}})} \times 100 \tag{S9}$$

where $A_{initial\ aggregates}$ and $A_{final\ aggregates}$ correspond to the SE-HPLC peak area of IgG aggregates of the initial complex media (before being in contact with the material) and aqueous solutions (after contact with the material), respectively.

Sodium dodecyl sulphate polyacrylamide gel electrophoresis (SDS-PAGE)

Sodium dodecyl sulphate polyacrylamide gel electrophoresis (SDS-PAGE) assays were performed to evaluate the protein profile in the initial and extracted samples. Samples were diluted 1:1 in Laemmli loading buffer (4% (*w/v*) SDS, 20 % (*v/v*) glycerol, 120 mM Tris-HCl pH 6.8, 100 mM dithiothreitol, 0.02 % (*w/v*) bromophenol blue), and denatured by incubation at 95 °C for 5 min. A volume of 20 µL of each sample was injected as follows: sera and samples derived from SILs purification processes were diluted 1:5 while IgG and HSA standards were injected, respectively, at 0.47 $mg \cdot mL^{-1}$ and 0.5 $mg \cdot mL^{-1}$. The protein molecular weight marker injected was the NZYColour Protein marker I (Nzytech, Lisboa, Portugal). Samples were run on precast Tris-glycine 12% polyacrylamide gels in a Mini Gel Tank (Novex, Invitrogen-ThermoFisher Scientific, Waltham, MA, USA) at 100 v during approximately 1h30. Lastly, protein staining was achieved by incubation with Bluesafe (Nzytech, Lisboa, Portugal) under mild agitation for 1h.

Optimization of the purification process by factorial design experiments

Equations used for the optimization of the purification process by factorial design experiments

The experimental data was treated according to second order polynomial Eq. (S10):

$$y = \beta_0 + \beta_i X_i + \beta_j X_j + \beta_{ii} X_i^2 + \beta_{jj} X_j^2 + \beta_{ij} X_i X_j \tag{S10}$$

where y is the dependent variable, namely the IgG yield or purity, and β_0, β_i, β_j, β_{ii}, β_{jj} and β_{ij} are the regression coefficients used respectively, to the intersection, linear, quadratic, and interaction of the terms. X_i and X_j represent the independent variables in the 2^k factorial planning. The experimental design involves the combination of three factors (independent variables) at two-levels. The number of runs (N) of each experiment is given by the Eq. (S11):

$$N = 2^k + 2k + Cx \tag{S11}$$

where 2^k is the number of factorial readings, 2k the number of axial readings and Cx a random number of repetitions of the central point which is expected to be closer to the best process operation conditions. It is very important to have several readings for the central point, to know the residual graph and, consequently, the standard deviation and the reproducibility quality of the experiment. On the other hand, the axial points are added to adjust the experience. Given the conditions and the number of independent variables to be studied, the Central Composite Rotatable Design was chosen, and the axial points calculated according to the value of α through the Eq. (S12):

$$\alpha = (2^k)\frac{1}{4} \tag{S12}$$

where ± α is the distance between the central and axial points.

Table S1. Factors tested and experimental Central Composite Rotatable Design levels.

	Axial Point	Factorial Point	Central Point	Factorial Point	Axial Point
	-1.68	**-1**	**0**	**1**	**1.68**
Contact time (min)	9.6	30.0	60.0	90.0	110.4
pH	1.6	3.0	5.0	7.0	8.4
S:L ratio ($mg{\cdot}mL^{-1}$)	16.0	50.0	100.0	150.0	184.0

Table S2. Factors tested and experimental Central Composite Rotatable Design levels for each system (coded and uncoded).

	Coded coefficients			Uncoded coefficients		
System	**Contact time (min)**	**pH**	**S:L ratio ($mg{\cdot}mL^{-1}$)**	**Contact time (min)**	**pH**	**S:L ratio ($mg{\cdot}mL^{-1}$)**
1	-1	-1	-1	30.0	3	50.0
2	1	-1	-1	90.0	3	50.0
3	-1	1	-1	30.0	7	50.0
4	1	1	-1	90.0	7	50.0
5	-1	-1	1	30.0	3	150.0
6	1	-1	1	90.0	3	150.0
7	-1	1	1	30.0	7	150.0
8	1	1	1	90.0	7	150.0
9	-1.68	0	0	9.6	5	100.0
10	1.68	0	0	110.4	5	100.0
11	0	-1.68	0	60.0	1.64	100.0
12	0	1.68	0	60.0	8.36	100.0
13	0	0	-1.68	60.0	5	16.0
14	0	0	1.68	60.0	5	184.0
15	0	0	0	60.0	5	100.0
16	0	0	0	60.0	5	100.0
17	0	0	0	60.0	5	100.0

Table S3. Performance parameters (%Yield$_{IgG}$ and %Purity$_{IgG}$) regarding IgG antibodies recovery and purification from human serum, after contact with [Si][C$_3$mim]Cl (results in the aqueous medium), [Si][N$_{3444}$]Cl and [Si][N$_{3888}$]Cl (results in the materials). The best result for each SIL is highlighted in bold.

System conditions			[Si][C$_3$mim]Cl		[Si][N$_{3444}$]Cl		[Si][N$_{3888}$]Cl	
Contact time (min)	**pH**	**S:L ratio (mg·mL^{-1})**	**%Yield$_{IgG}$**	**%Purity$_{IgG}$**	**%Yield$_{IgG}$**	**%Purity$_{IgG}$**	**%Yield$_{IgG}$**	**%Purity$_{IgG}$**
30.0	3	50.0	100.0	45.8	10.0	53.2	0.0	0.0
90.0	3	50.0	**100.0**	**46.9**	0.0	0.0	0.0	0.0
30.0	7	50.0	63.3	42.2	24.5	80.5	35.3	66.7
90.0	7	50.0	68.3	42.7	13.8	72.5	**42.8**	**81.1**
30.0	3	150.0	100.0	43.6	45.1	55.3	25.7	24.8
90.0	3	150.0	97.2	42.8	0.0	0.0	26.2	28.7
30.0	7	150.0	58.7	46.4	**57.0**	**65.0**	67.3	59.9
90.0	7	150.0	58.7	45.0	52.0	55.8	65.5	57.7
9.6	5	100.0	84.9	40.4	33.5	57.4	34.4	45.5
110.4	5	100.0	86.8	40.8	30.6	53.8	47.2	42.7
60.0	1.64	100.0	100.0	42.6	0.0	0.0	16.8	22.4
60.0	8.36	100.0	70.5	37.6	26.4	93.3	48.2	52.7
60.0	5	16.0	86.4	42.1	12.6	85.8	22.8	43.5
60.0	5	184.0	80.0	39.4	12.5	97.8	47.6	39.3
60.0	5	100.0	88.6	42.2	15.9	98.3	48.0	43.7
60.0	5	100.0	84.0	40.4	10.4	97.4	45.3	42.4
60.0	5	100.0	86.5	41.2	15.2	98.2	36.2	46.0

Assessment of IgG stability and anti-IL-8 mAbs activity

Circular Dichroism

Circular dichroism was used to appraise any changes in the secondary structure of IgG (0.47 mg × mL^{-1}) caused by the pH of the buffers used for adsorption, as well as in the flowthrough (diluted at 1:20 (*v:v*)) following the preferential adsorption of HSA in [Si][C_3mim]Cl. Spectra of HSA (0.1 mg × mL^{-1}) and the 1:20 diluted human serum (further diluted to 1:400 (*v:v*)) were also acquired for comparison purposes.

CD spectra were recorded using a Jasco J-815 CD spectrometer at constant temperature (25 °C) using a scanning speed of 20 nm/min, with a response time of 1s in the far-UV region (195-260 nm). The recording bandwith was of 2 nm with a step size of 1 nm using a quartz cell with an optical path length of 1 mm. Three scans were averaged per spectrum to improve the signal-to-noise ratio, and the baseline established with the appropriate buffer.

Competitive enzyme linked immunosorbent assays (ELISA)

Competitive enzyme linked immunosorbent assays (ELISA) were performed for the CHO cell culture supernatants and the flowthrough obtained from [Si][C_3mim]Cl to qualitatively evaluate the activity of anti-human IL-8 mABs after the studied purification processes. The assay was conducted using a 96-well ELISA plate from a Quantikine® Human IL-8/CXCL8 kit from R&D systems (Minnneapolis, MN, USA) with some modifications from the manufacturer's instructions, as detailed below. The plate was coated with 100 μL assay diluent followed by the addition of 50 μL of 1 mg·L^{-1} of human IL-8 standard from Sigma-Aldrich-Merck KGaA (St Louis, Missouri, USA). The plate was left for incubating for 2 h at room temperature.

After this period, each well was aspirated and washed for four consecutive times with wash buffer. Then, 100 μL of each sample containing anti-IL-8 mAbs was added to the wells, and were left to incubate for 1 h at room temperature, being further washed as previously described. Mouse anti-human CXCL8/IL8 antibody 1 mg × mL^{-1} (RayBiotech Life, Peachtree Corners, GA, USA) was used as the positive control, while the calibrator diluent RD5P included in the kit was used as the negative control. 100 μL of anti-IL-8 conjugate was added to all wells and incubated for 1 h at room temperature, and after washed again as previously described. 200 μL of substrate solution was then added to the wells and incubated for 10 min at room temperature (protected from the light with a plate sealer).

Finally, 50 μL of stop solution was added to end the reaction, and the absorbance was measured at 450 nm and 540 nm in a BioTek SYNERGY|HT microplate reader. Final results were calculated based on the subtraction of the absorbance at 450 nm for the obtained at 570 nm, to correct optical deviations from the plate. In general, a decrease in absorbance was indicative of the presence of anti-human IL-8 mAbs with biological activity.

Results and discussion

Synthesis and characterization of SIL materials

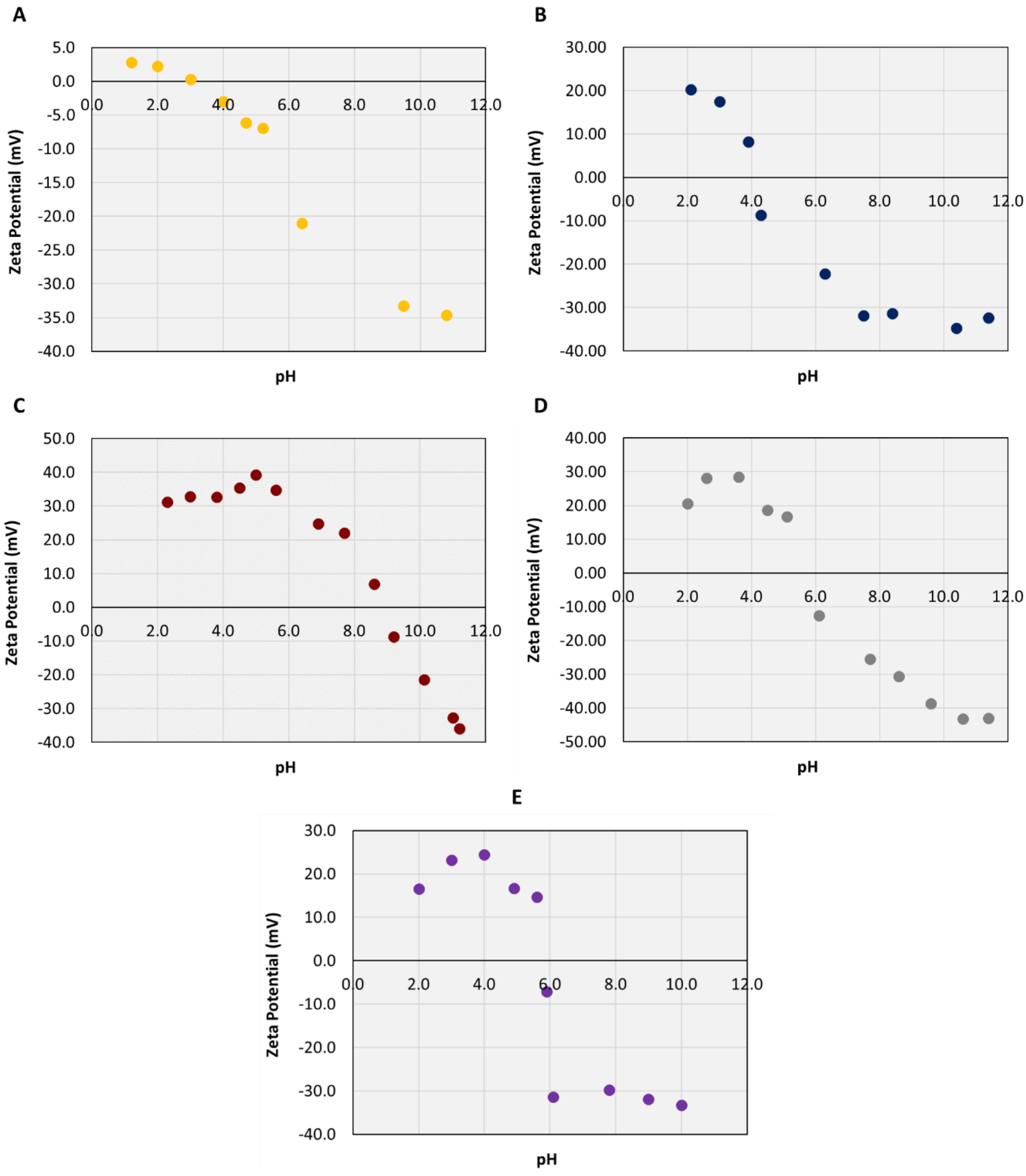

Fig. S2. Representation of the zeta potential as a function of the pH for: (A) activated silica; (B) [Si][C_3]Cl; (C) [Si][C_3mim]Cl; (D) [Si][N_{3444}]Cl; and (E) [Si][N_{3888}]Cl.

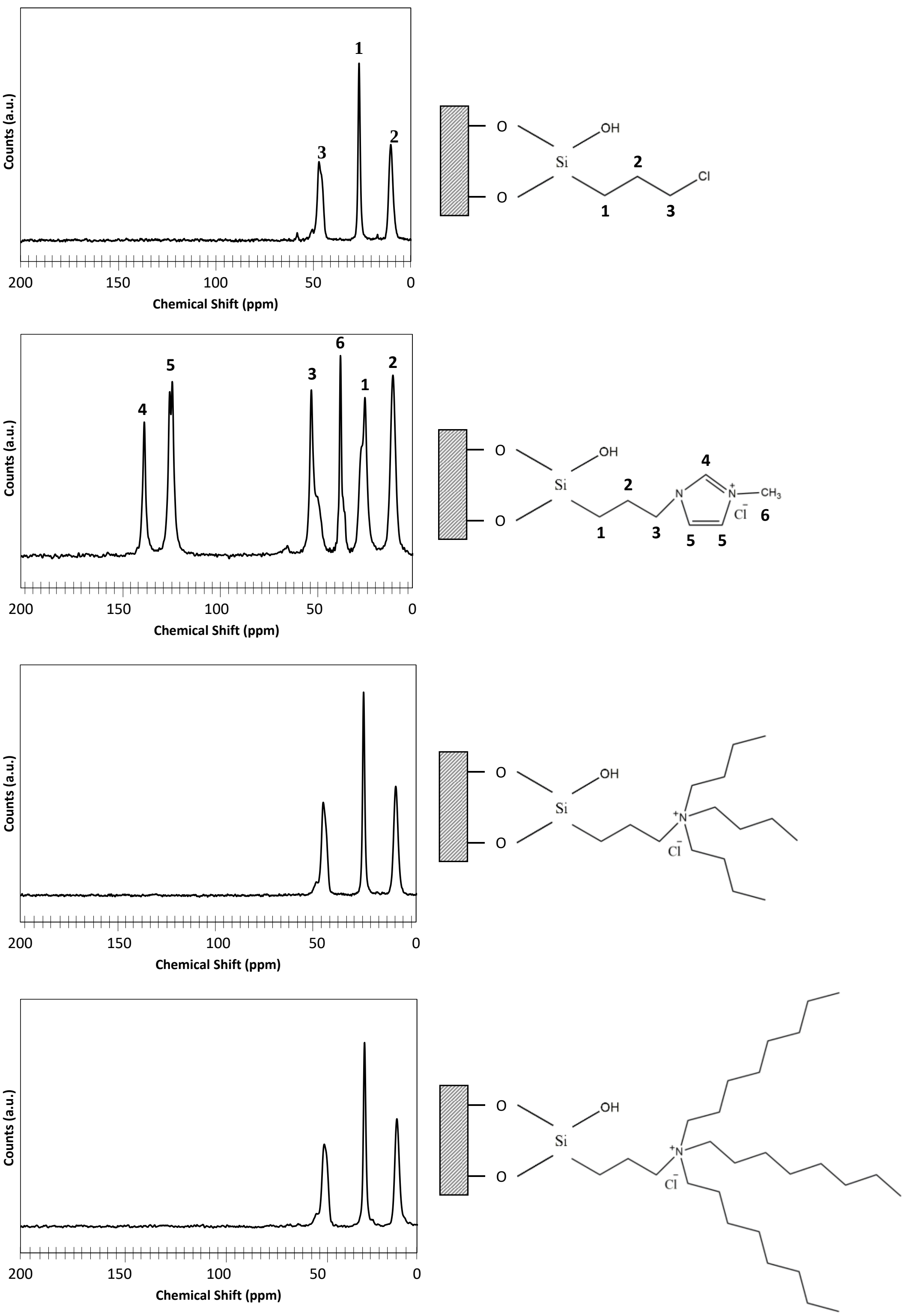

Fig. S3. Solid-state ^{13}C NMR spectra of [Si][C_3]Cl and SILs ([Si][C_3mim]Cl, [Si][N_{3444}]Cl and [Si][N_{3888}]Cl).

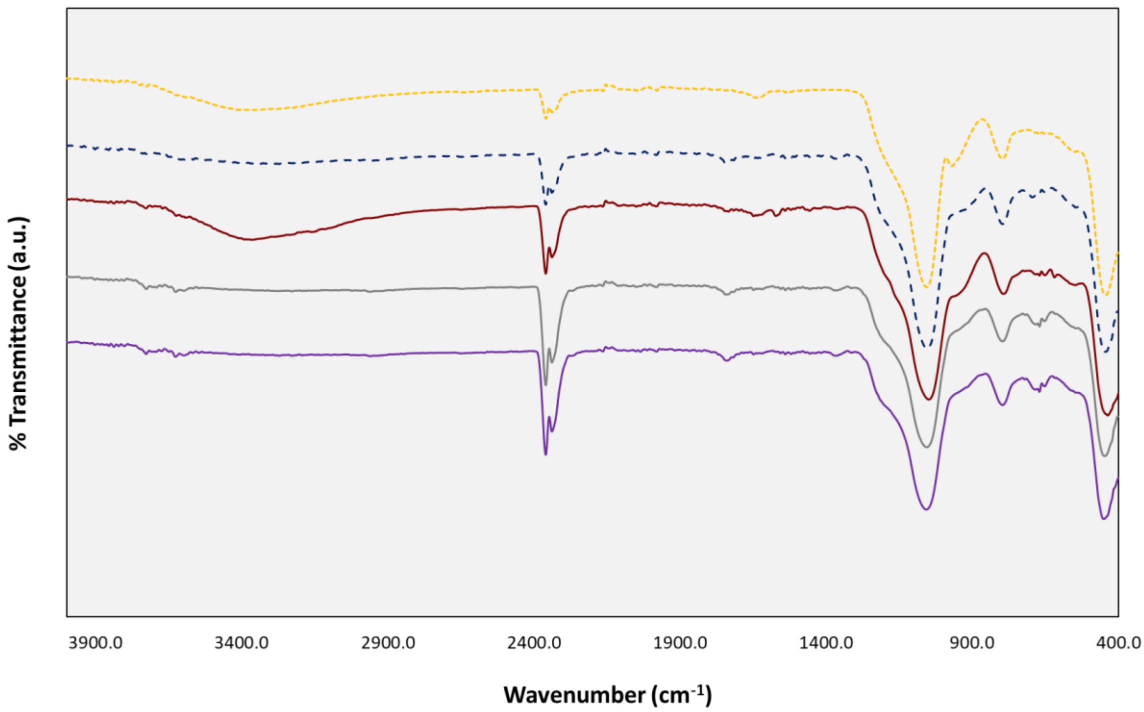

Fig. S4. ATR-FTIR spectra of the different materials under study: activated silica (··); [Si][C_3]Cl (--); [Si][C_3mim]Cl (–); [Si][N_{3444}]Cl (–); and [Si][N_{3888}]Cl (–).

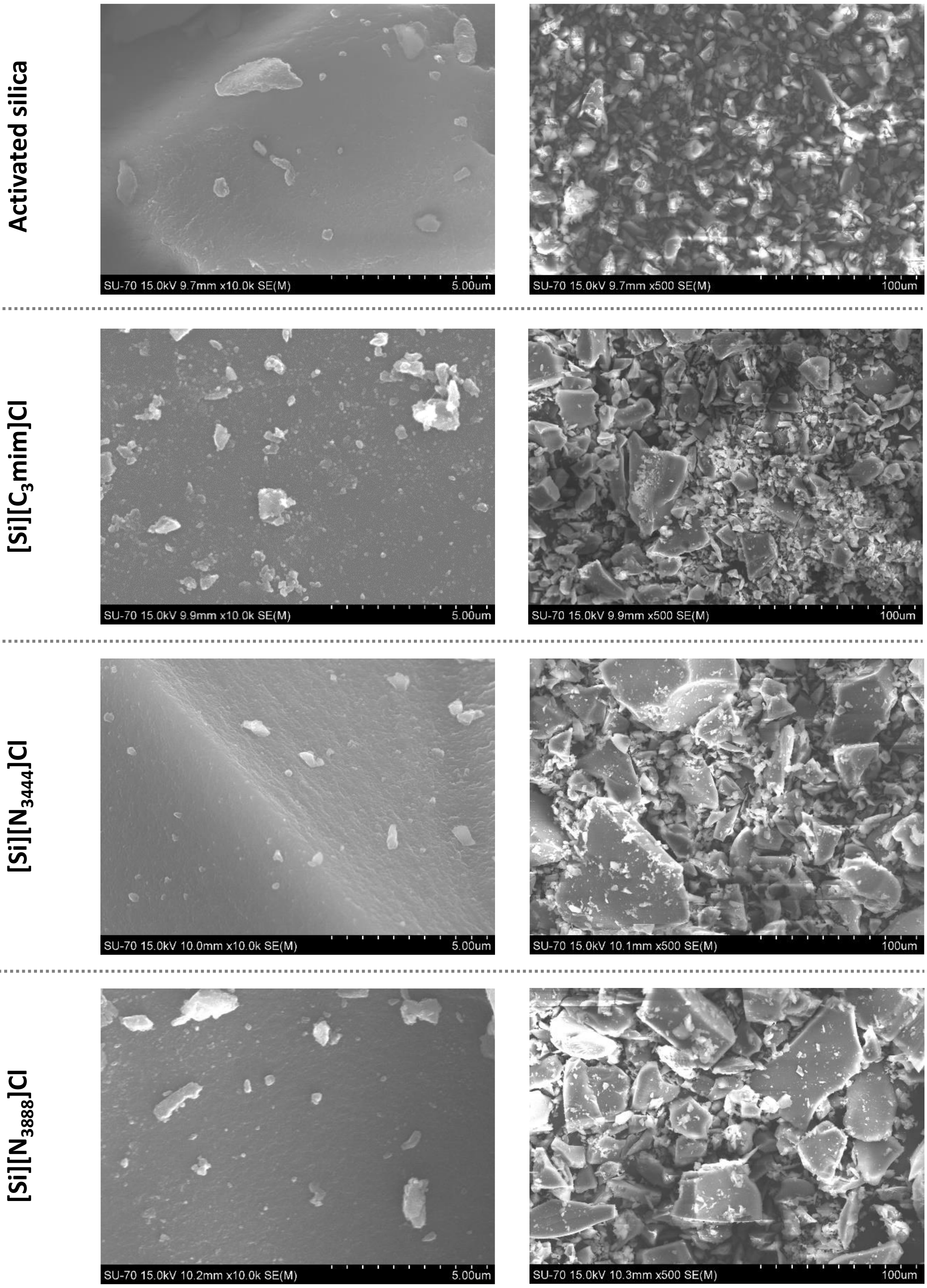

Fig. S5. SEM images of the activated silica and synthesized SILs ([Si][C_3mim]Cl, [Si][N_{3444}]Cl and [Si][N_{3888}]Cl) at two different magnifications: 10000 × (right images) and 500 × (left images).

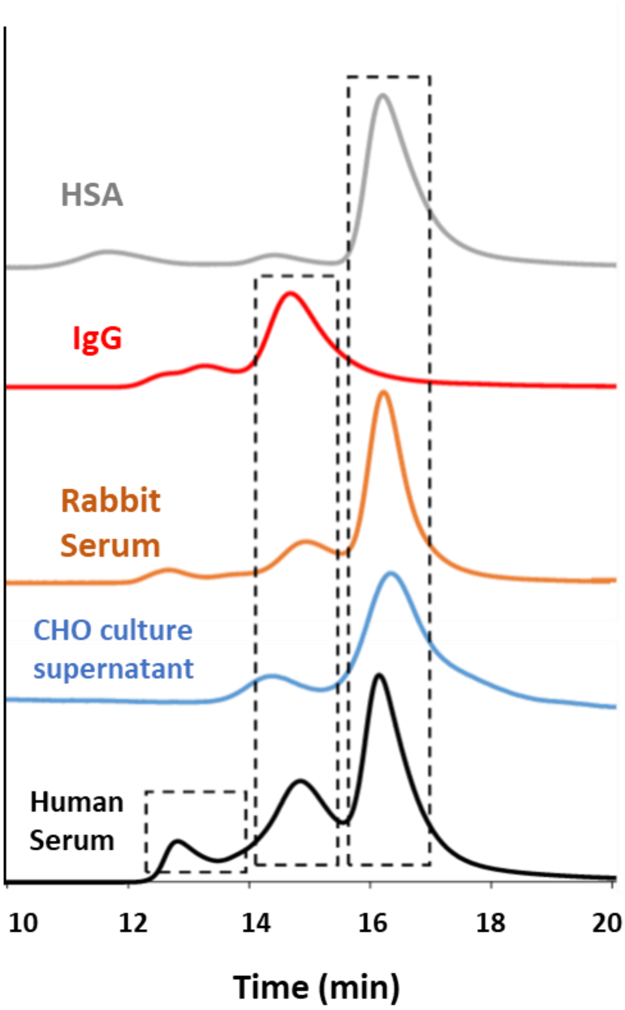

Fig. S6. Characterization of the complex biological matrices studied in this work: SE-HPLC chromatograms of pure IgG solution 100 mg·L^{-1} (—), pure HSA solution 200 mg·L^{-1} (—), human serum (—), CHO cell culture supernatant (—), and rabbit serum (—).

Optimization of the adsorption process and selectivity by factorial design experiments

Table S4. Data attributed to the independent variables (S:L ratio, pH and contact time) to define the 2^3 factorial planning and respective experimental results of recovery yield of IgG using [Si][C_3mim]Cl, theoretical results of the developed mathematical model and respective relative deviation.

System	S:L ratio ($mg \cdot mL^{-1}$)	pH	Contact time (min)	%$Yield_{IgG}$ experimental	%$Yield_{IgG}$ theoretical	Residues
1	50.0	3	30.0	100.0	97.0	3.0
2	50.0	3	90.0	100.0	97.8	2.2
3	50.0	7	30.0	63.3	69.0	-5.6
4	50.0	7	90.0	68.3	73.6	-5.3
5	150.0	3	30.0	100.0	97.8	2.3
6	150.0	3	90.0	97.2	94.6	2.5
7	150.0	7	30.0	58.7	64.0	-5.3
8	150.0	7	90.0	58.7	64.7	-6.1
9	100.0	5	9.6	84.9	83.0	1.9
10	100.0	5	110.4	86.7	84.3	2.5
11	100.0	1.64	60.0	100.0	107.4	-7.4
12	100.0	8.36	60.0	70.5	58.7	11.8
13	16.0	5	60.0	86.4	84.4	2.0
14	184.0	5	60.0	80.0	77.6	2.4
15	100.0	5	60.0	88.6	86.6	2.0
16	100.0	5	60.0	84.0	86.6	-2.6
17	100.0	5	60.0	86.5	86.6	-0.2

Table S5. Regression coefficients of the predicted second-order polynomial model for the recovery yield of IgG with [Si][C_3mim]Cl.

	Regression coefficients	Standard deviation	t-student (7)	p - value
Interception	99.8	29.4	3.4	0.0
S:L ratio	0.2	0.2	0.9	0.4
S:L ratio^2	0.0	0.0	-0.9	0.4
pH	-3.6	6.6	-0.6	0.6
pH^2	-0.3	0.5	-0.6	0.6
Time	0.1	0.4	0.3	0.7
Time^2	0.0	0.0	-0.5	0.6
S:L ratio × pH	-0.0	0.0	-0.6	0.6
S:L ratio × Time	0.0	0.0	-0.4	0.7
pH × Time	0.0	0.0	0.4	0.7

Table S6. ANOVA data for the recovery yield of IgG, obtained from the factorial planning carried with [Si][C_3mim]Cl.

	Sum Squares (SS)	Degrees of Freedom	Mean Square	Fcal	p - value
S:L ratio	57.0	1.0	57.0	1.1	0.3
S:L ratio^2	44.8	1.0	44.8	0.8	0.4
pH	2865.6	1.0	2865.6	53.7	0.0
pH^2	18.0	1.0	18.0	0.3	0.6
Time	2.1	1.0	2.1	0.0	0.9
Time^2	12.9	1.0	12.9	0.2	0.6
S:L ratio × pH	16.4	1.0	16.4	0.3	0.6
S:L ratio × Time	7.6	1.0	7.6	0.1	0.7
pH × Time	7.6	1.0	7.6	0.1	0.7
Error	373.7	7.0	53.4		
Total SS	3381.8	16.0			

Table S7. Data attributed to the independent variables (S:L ratio, pH and contact time) to define the 2^3 factorial planning and respective experimental results of purity of IgG using [Si][C_3mim]Cl, theoretical results of the developed mathematical model and respective relative deviation.

System	S:L ratio ($mg \cdot mL^{-1}$)	pH	Contact time (min)	%$Purity_{IgG}$ experimental	%$Purity_{IgG}$ theoretical	Residues
1	50.0	3	30.0	45.8	45.0	0.9
2	50.0	3	90.0	46.9	46.2	0.7
3	50.0	7	30.0	42.2	40.4	1.8
4	50.0	7	90.0	42.7	41.1	1.6
5	150.0	3	30.0	43.6	42.1	1.6
6	150.0	3	90.0	42.8	41.4	1.4
7	150.0	7	30.0	46.4	43.9	2.5
8	150.0	7	90.0	45.0	42.7	2.3
9	100.0	5	9.6	40.4	42.8	-2.4
10	100.0	5	110.4	40.8	42.8	-2.1
11	100.0	1.64	60.0	42.6	43.7	-1.1
12	100.0	8.36	60.0	37.6	41.0	-3.4
13	16.0	5	60.0	42.1	43.5	-1.4
14	184.0	5	60.0	39.4	42.5	-3.1
15	100.0	5	60.0	42.2	41.0	1.2
16	100.0	5	60.0	40.4	41.0	-0.6
17	100.0	5	60.0	41.2	41.0	0.2

Table S8. Regression coefficients of the predicted second-order polynomial model for the purity of IgG with [Si][C_3mim]Cl.

	Regression coefficients	Standard deviation	t-student (7)	p - value
Interception	57.6	11.7	4.9	0.0
S:L ratio	-0.1	0.1	-1.3	0.2
S:L ratio^2	0.0	0.0	0.8	0.4
pH	-3.1	2.6	-1.2	0.3
pH^2	0.1	0.2	0.6	0.6
Time	-0.0	0.2	-0.3	0.8
Time^2	0.0	0.0	0.8	0.5
S:L ratio × pH	0.0	0.0	1.6	0.2
S:L ratio × Time	0.0	0.0	-0.5	0.7
pH × Time	0.0	0.0	-0.1	0.9

Table S9. ANOVA data for the purity of IgG, obtained from the factorial planning carried with [Si][C_3mim]Cl.

	Sum Squares (SS)	Degrees of Freedom	Mean Square	Fcal	p - value
S:L ratio	1.3	1.0	1.3	0.2	0.7
S:L ratio^2	5.8	1.0	5.8	0.7	0.4
pH	9.2	1.0	9.2	1.1	0.3
pH^2	2.6	1.0	2.6	0.3	0.6
Time	0.0	1.0	0.0	0.0	1.0
Time^2	4.8	1.0	4.8	0.6	0.5
S:L ratio × pH	20.7	1.0	20.7	2.5	0.2
S:L ratio × Time	1.8	1.0	1.8	0.2	0.7
pH × Time	0.2	1.0	0.2	0.0	0.9
Error	58.8	7.0	8.4		
Total SS	100.4	16.0			

Table S10. Data attributed to the independent variables (S:L ratio, pH and contact time) to define the 2^3 factorial planning and respective experimental results of recovery yield of IgG using [Si][N_{3444}]Cl, theoretical results of the developed mathematical model and respective relative deviation.

System	S:L ratio ($mg{\cdot}mL^{-1}$)	pH	Contact time (min)	$\%Yield_{IgG}$ experimental	$\%Yield_{IgG}$ theoretical	Residues
1	50.0	3	30.0	10.0	16.6	-6.5
2	50.0	3	90.0	0.0	2.9	-2.9
3	50.0	7	30.0	24.5	17.8	6.7
4	50.0	7	90.0	13.8	23.9	-10.1
5	150.0	3	30.0	45.1	30.5	14.6
6	150.0	3	90.0	0.0	2.2	-2.2
7	150.0	7	30.0	57.0	49.5	7.5
8	150.0	7	90.0	52.0	41.0	11.1
9	100.0	5	9.6	33.5	44.5	-11.1
10	100.0	5	110.4	30.6	25.9	4.7
11	100.0	1.64	60.0	0.0	-0.4	0.4
12	100.0	8.36	60.0	26.4	33.2	-6.8
13	16.0	5	60.0	12.6	2.8	9.8
14	184.0	5	60.0	12.5	28.8	-16.3
15	100.0	5	60.0	15.9	13.4	2.4
16	100.0	5	60.0	10.4	13.4	-3.1
17	100.0	5	60.0	15.2	13.4	1.8

Table S11. Regression coefficients of the predicted second-order polynomial model for the recovery yield of IgG with [Si][N_{3444}]Cl.

	Regression coefficients	Standard deviation	t-student (7)	p - value
Interception	57.1	51.9	1.1	0.3
S:L ratio	0.0	0.4	0.0	1.0
S:L ratio^2	0.0	0.0	0.2	0.8
pH	-7.0	11.7	-0.6	0.6
pH^2	0.3	1.0	0.3	0.8
Time	-1.4	0.7	-1.9	0.1
Time^2	0.0	0.0	2.0	0.1
S:L ratio × pH	0.0	0.1	1.0	0.4
S:L ratio × Time	0.0	0.0	-0.8	0.5
pH × Time	0.1	0.1	1.1	0.3

Table S12. ANOVA data for the recovery yield of IgG, obtained from the factorial planning carried with [Si][N_{3444}]Cl.

	Sum Squares (SS)	Degrees of Freedom	Mean Square	Fcal	p - value
S:L ratio	816.7	1.0	816.7	4.9	0.1
S:L ratio^2	7.7	1.0	7.7	0.1	0.8
pH	1368.2	1.0	1368.2	8.2	0.0
pH^2	12.5	1.0	12.5	0.1	0.8
Time	419.5	1.0	419.5	2.5	0.2
Time^2	669.0	1.0	669.0	4.0	0.1
S:L ratio × pH	159.0	1.0	159.0	1.0	0.4
S:L ratio × Time	107.7	1.0	107.7	0.7	0.5
pH × Time	194.3	1.0	194.3	1.2	0.3
Error	1165.1	7.0	166.4		
Total SS	4935.4	16.0			

Table S13. Data attributed to the independent variables (S:L ratio, pH and contact time) to define the 2^3 factorial planning and respective experimental results of purity of IgG using $[Si][N_{3444}]Cl$, theoretical results of the developed mathematical model and respective relative deviation.

System	S:L ratio ($mg{\cdot}mL^{-1}$)	pH	Contact time (min)	$\%Purity_{IgG}$ experimental	$\%Purity_{IgG}$ theoretical	Residues
1	50.0	3	30.0	53.2	47.2	6.1
2	50.0	3	90.0	0.0	5.8	-5.8
3	50.0	7	30.0	80.5	80.1	0.4
4	50.0	7	90.0	72.5	84.5	-11.9
5	150.0	3	30.0	55.3	55.1	0.2
6	150.0	3	90.0	0.0	12.1	-12.1
7	150.0	7	30.0	65.0	70.9	-5.9
8	150.0	7	90.0	55.8	73.6	-17.8
9	100.0	5	9.6	57.4	63.5	-6.1
10	100.0	5	110.4	53.8	31.0	22.7
11	100.0	1.64	60.0	0.0	-1.3	1.3
12	100.0	8.36	60.0	93.3	78.0	15.4
13	16.0	5	60.0	85.8	84.7	1.1
14	184.0	5	60.0	97.8	82.2	15.6
15	100.0	5	60.0	98.3	98.9	-0.7
16	100.0	5	60.0	97.4	98.9	-1.6
17	100.0	5	60.0	98.2	98.9	-0.7

Table S14. Regression coefficients of the predicted second-order polynomial model for the purity of IgG with [Si][N_{3444}]Cl.

	Regression coefficients	Standard deviation	t-student (7)	p - value
Interception	-134.7	63.6	-2.1	0.1
S:L ratio	0.7	0.5	1.2	0.3
S:L ratio^2	0.0	0.0	-1.2	0.3
pH	58.4	14.4	4.1	0.0
pH^2	-5.4	1.2	-4.6	0.0
Time	1.2	0.9	1.4	0.2
Time^2	-0.0	0.0	-3.9	0.0
S:L ratio × pH	-0.0	0.1	-0.8	0.5
S:L ratio × Time	0.0	0.0	-0.1	0.9
pH × Time	0.2	0.01	2.0	0.1

Table S15. ANOVA data for the purity of IgG, obtained from the factorial planning carried with [Si][N_{3444}]Cl.

	Sum Squares (SS)	Degrees of Freedom	Mean Square	Fcal	p - value
S:L ratio	7.3	1.0	7.3	0.0	0.9
S:L ratio^2	337.3	1.0	337.3	1.4	0.3
pH	7601.4	1.0	7601.4	30.4	0.0
pH^2	5183.7	1.0	5183.7	20.7	0.0
Time	1274.5	1.0	1274.5	5.1	0.1
Time^2	3768.6	1.0	3768.6	15.1	0.0
S:L ratio × pH	147.6	1.0	147.6	0.6	0.5
S:L ratio × Time	1.4	1.0	1.4	0.0	0.9
pH × Time	1043.8	1.0	1043.8	4.2	0.1
Error	1751.9	7.0	250.3		
Total SS	18945.9	16.0			

Table S16. Data attributed to the independent variables (S:L ratio, pH and contact time) to define the 2^3 factorial planning and respective experimental results of recovery yield of IgG using [Si][N_{3888}]Cl, theoretical results of the developed mathematical model and respective relative deviation.

System	S:L ratio ($mg \cdot mL^{-1}$)	pH	Contact time (min)	%$Yield_{IgG}$ experimental	%$Yield_{IgG}$ theoretical	Residues
1	50.0	3	30.0	0.0	5.5	-5.5
2	50.0	3	90.0	0.0	10.4	-10.4
3	50.0	7	30.0	35.3	34.5	0.8
4	50.0	7	90.0	42.8	42.0	0.7
5	150.0	3	30.0	25.7	28.7	-3.0
6	150.0	3	90.0	26.2	29.3	-3.1
7	150.0	7	30.0	67.3	59.1	8.1
8	150.0	7	90.0	65.5	62.3	3.2
9	100.0	5	9.6	34.4	35.8	-1.4
10	100.0	5	110.4	47.2	42.6	4.6
11	100.0	1.64	60.0	16.8	4.8	12.0
12	100.0	8.36	60.0	48.2	56.9	-8.8
13	16.0	5	60.0	22.8	15.3	7.5
14	184.0	5	60.0	47.6	51.8	-4.2
15	100.0	5	60.0	48.0	43.4	4.7
16	100.0	5	60.0	45.3	43.4	2.0
17	100.0	5	60.0	36.2	43.4	-7.2

Table S17. Regression coefficients of the predicted second-order polynomial model for the recovery yield of IgG with [Si][N_{3888}]Cl.

	Regression coefficients	Standard deviation	t-student (7)	p - value
Interception	-68.1	38.1	-1.8	0.1
S:L ratio	0.5	0.3	1.7	0.1
S:L ratio^2	0.0	0.0	-1.2	0.3
pH	17.8	8.6	2.1	0.1
pH^2	-1.1	0.7	-1.6	0.2
Time	0.3	0.5	0.5	0.6
Time^2	0.0	0.0	-0.5	0.6
S:L ratio × pH	0.0	0.0	0.1	0.9
S:L ratio × Time	0.0	0.0	-0.3	0.8
pH × Time	0.0	0.1	0.2	0.9

Table S18. ANOVA data for the recovery yield of IgG, obtained from the factorial planning carried with [Si][N_{3888}]Cl.

	Sum Squares (SS)	Degrees of Freedom	Mean Square	Fcal	p - value
S:L ratio	1612.3	1.0	1612.3	17.9	0.004
S:L ratio^2	135.7	1.0	135.7	1.5	0.3
pH	3280.2	1.0	3280.2	36.5	0.0005
pH^2	220.1	1.0	220.1	2.5	0.2
Time	56.2	1.0	56.2	0.6	0.5
Time^2	24.6	1.0	24.6	0.3	0.6
S:L ratio × pH	01.0	1.0	1.0	0.0	0.9
S:L ratio × Time	9.6	1.0	9.6	0.1	0.8
pH × Time	3.3	1.0	3.3	0.0	0.9
Error	629.8	7.0	90.0		
Total SS	5871.9	16.0			

Table S19. Data attributed to the independent variables (S:L ratio, pH and contact time) to define the 2^3 factorial planning and respective experimental results of purity of IgG using [Si][N_{3888}]Cl, theoretical results of the developed mathematical model and respective relative deviation.

System	S:L ratio ($mg \cdot mL^{-1}$)	pH	Contact time (min)	$\%Purity_{IgG}$ experimental	$\%Purity_{IgG}$ theoretical	Residues
1	50.0	3	30.0	0.0	7.9	-7.9
2	50.0	3	90.0	0.0	10.7	-10.7
3	50.0	7	30.0	66.7	65.3	1.4
4	50.0	7	90.0	81.1	72.2	8.9
5	150.0	3	30.0	24.8	34.4	-9.7
6	150.0	3	90.0	28.7	30.8	-2.1
7	150.0	7	30.0	59.9	50.0	10.0
8	150.0	7	90.0	57.7	50.5	7.2
9	100.0	5	9.6	45.5	42.2	3.4
10	100.0	5	110.4	42.7	45.0	-2.3
11	100.0	1.64	60.0	22.4	4.6	17.8
12	100.0	8.36	60.0	52.7	69.4	-16.7
13	16.0	5	60.0	43.5	38.9	4.6
14	184.0	5	60.0	39.3	42.8	-3.6
15	100.0	5	60.0	43.7	44.1	-0.4
16	100.0	5	60.0	42.4	44.1	-1.7
17	100.0	5	60.0	46.0	44.1	1.9

Table S20. Regression coefficients of the predicted second-order polynomial model for the purity of IgG with [Si][N_{3888}]Cl.

	Regression coefficients	Standard deviation	t-student (7)	p - value
Interception	-82.7	51.7	-1.6	0.2
S:L ratio	0.7	0.4	1.6	0.2
S:L ratio^2	0.0	0.0	-0.3	0.8
pH	25.4	11.7	2.2	0.1
pH^2	-0.6	1.0	-0.7	0.5
Time	0.1	0.7	0.1	0.9
Time^2	0.0	0.0	-0.1	1.0
S:L ratio × pH	-0.1	0.1	-2.3	0.1
S:L ratio × Time	0.0	0.0	-0.4	0.7
pH × Time	0.0	0.1	0.2	0.8

Table S21. ANOVA data for the purity of IgG, obtained from the factorial planning carried with [Si][N_{3888}]Cl.

	Sum Squares (SS)	Degrees of Freedom	Mean Square	Fcal	p - value
S:L ratio	19.0	1.0	19.0	0.1	0.7
S:L ratio^2	14.7	1.0	14.7	0.09	0.8
pH	5063.0	1.0	5063.0	30.6	0.0009
pH^2	71.0	1.0	71.0	0.4	0.5
Time	9.4	1.0	9.4	0.06	0.8
Time^2	0.4	1.0	0.4	0.002	1.0
S:L ratio × pH	875.5	1.0	875.5	5.3	0.06
S:L ratio × Time	20.4	1.0	20.4	0.1	0.7
pH × Time	8.4	1.0	8.4	0.05	0.8
Error	1158.8	7.0	165.6		
Total SS	7232.9	16.0			

Table S22. Predicted conditions for the optimal performance parameters (%Yield$_{IgG}$ and %Purity$_{IgG}$) for [Si][C_3mim]Cl, [Si][N_{3444}]Cl and [Si][N_{3888}]Cl.

SIL	Predicted optimal conditions			Performance parameters (%)	
	S:L ratio ($mg \cdot mL^{-1}$)	pH	Contact time (min)	Purity$_{IgG}$	Yield$_{IgG}$
[Si][C_3mim]Cl	70	5	70	-	> 85
	100	< 1	60	> 45	-
[Si][N_{3444}]Cl	100	> 9	60	-	> 70
	100	6	60	> 80	
[Si][N_{3888}]Cl	100	> 8	90	-	> 46
	100	> 9	60	> 70	-

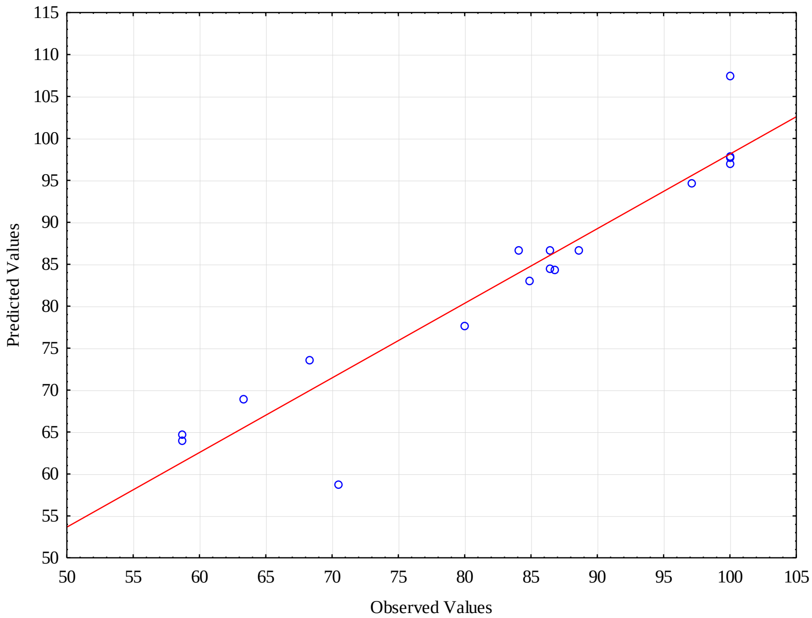

Fig. S6. Predicted *versus* observed values for the recovery yield of IgG from human serum using [Si][C_3mim]Cl.

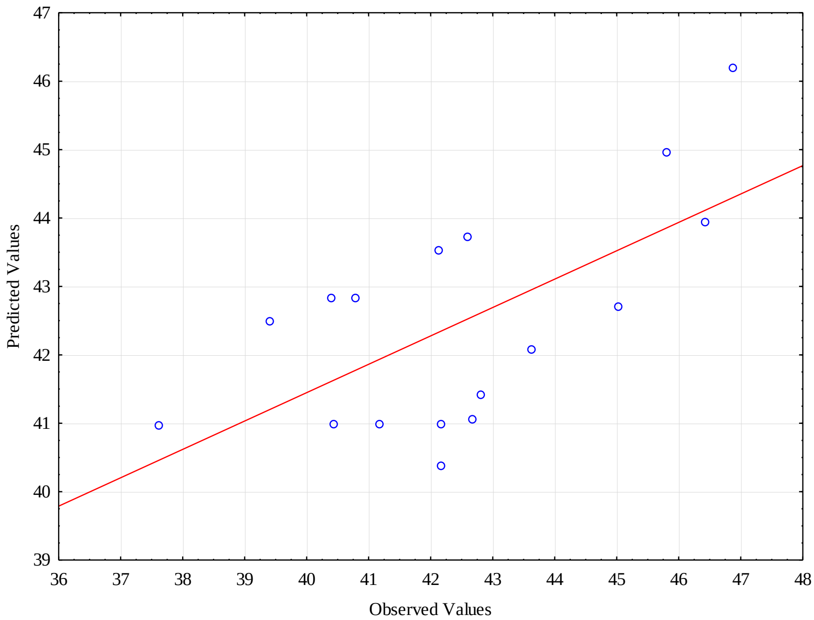

Fig. S7. Predicted *versus* observed values for the purity of IgG from human serum using [Si][C_3mim]Cl.

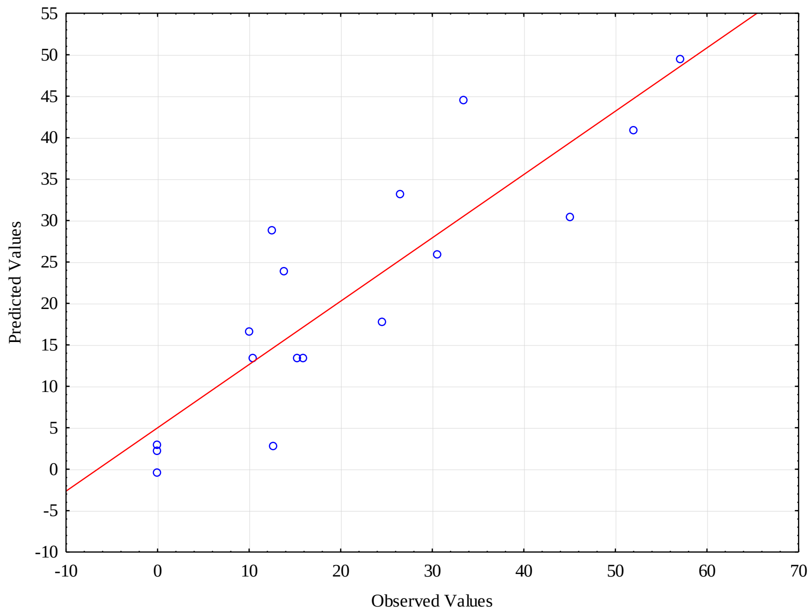

Fig. S8. Predicted *versus* observed values for the recovery yield of IgG from human serum using [Si][N_{3444}]Cl.

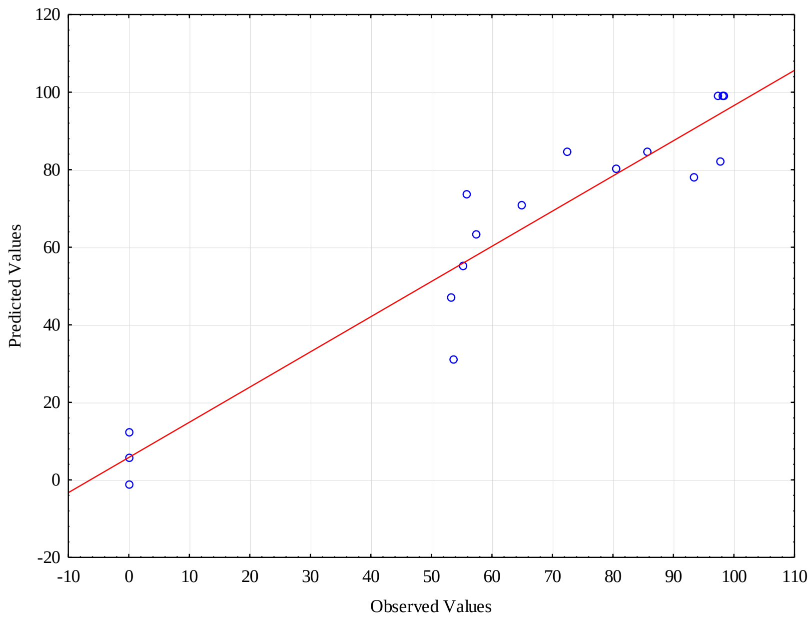

Fig. S9. Predicted *versus* observed values for the purity of IgG from human serum using [Si][N_{3444}]Cl.

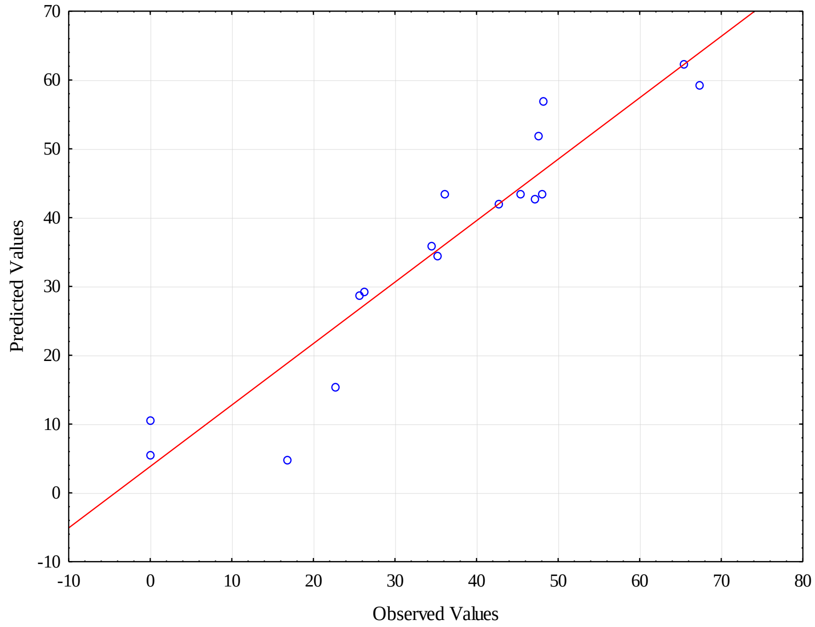

Fig. S10. Predicted *versus* observed values for the recovery yield of IgG from human serum using [Si][N_{3888}]Cl.

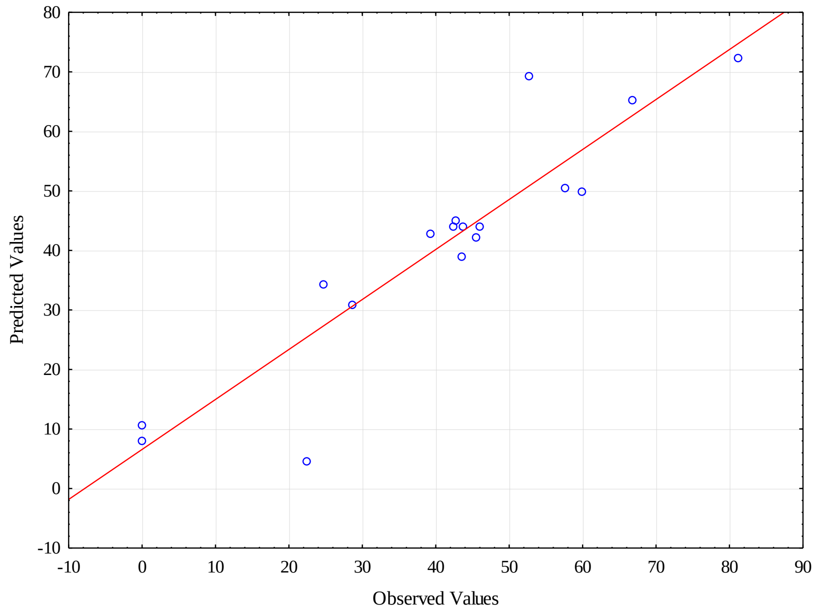

Fig. S11. Predicted *versus* observed values for the purity of IgG from human serum using [Si][N_{3888}]Cl.

(A)

(B)

(C)

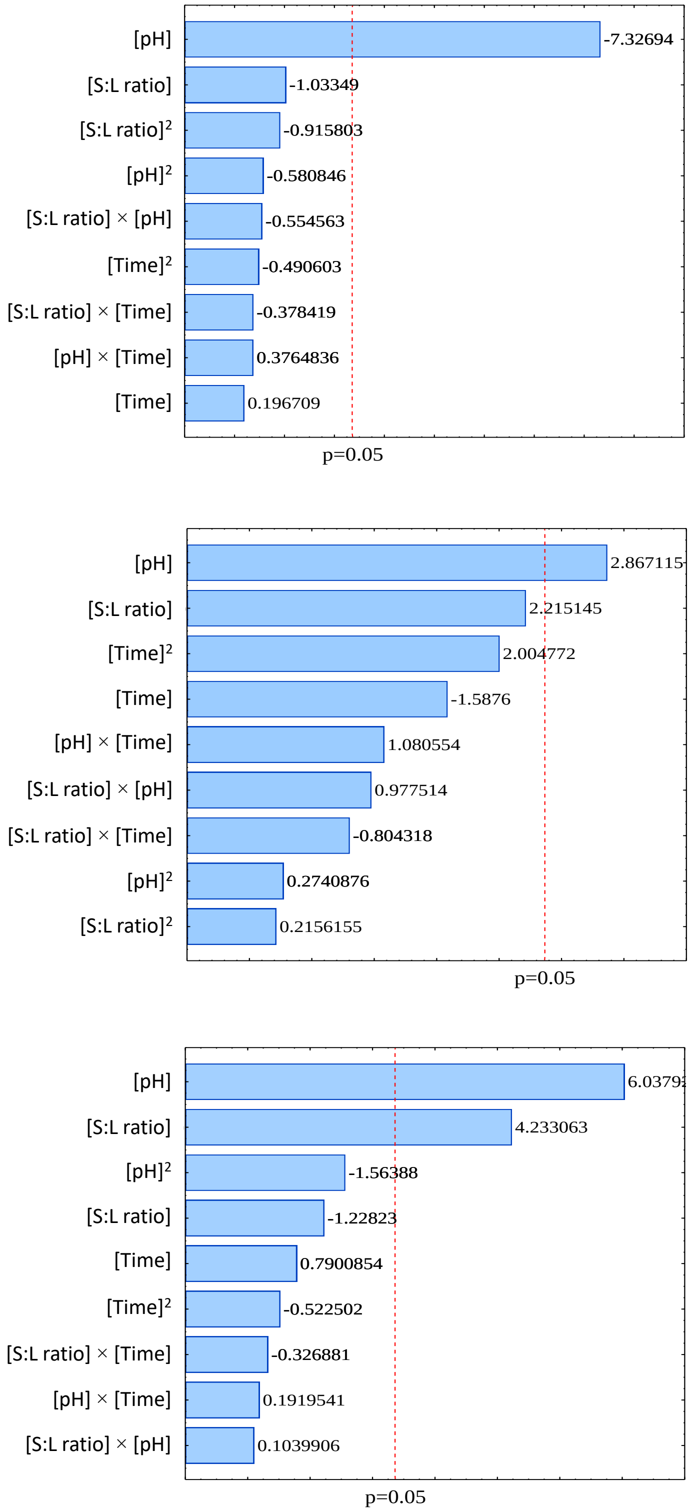

Fig. S12. Pareto charts obtained for the 2^3 factorial planning regarding the study of the IgG recovery yield using: (A) [Si][C_3mim]Cl; (B) [Si][N_{3444}]Cl; and (C) [Si][N_{3888}]Cl.

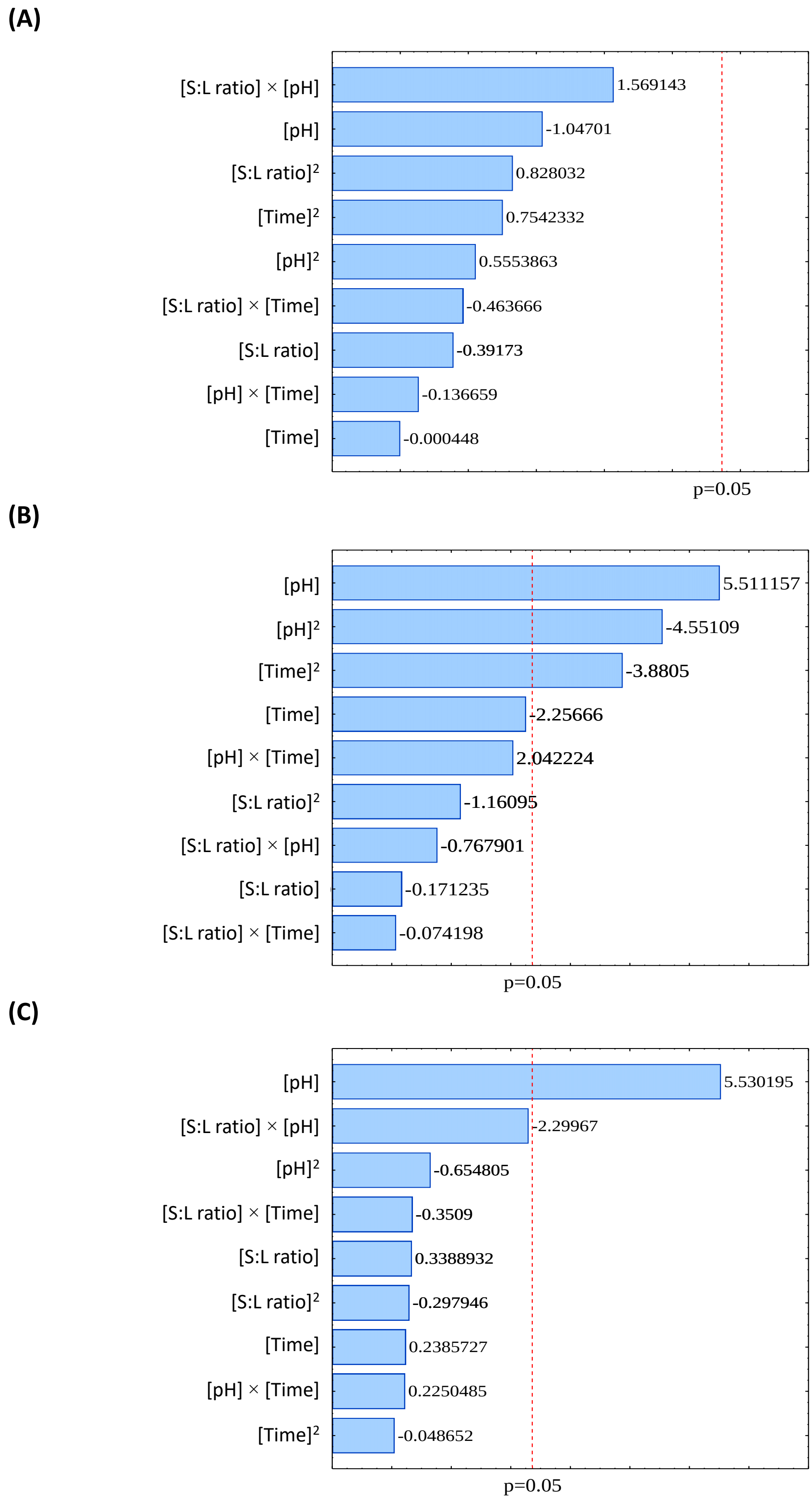

Fig. S13. Pareto charts obtained for the 2^3 factorial planning regarding the study of the IgG purity using: (A) [Si][C_3mim]Cl; (B) [Si][N_{3444}]Cl; and (C) [Si][N_{3888}]Cl.

Experimental optimization of the IgG downstream process

Table S23. Performance parameters ([IgG], %Yield$_{IgG}$, %Purity$_{IgG}$ and %Aggregation$_{IgG}$) regarding IgG antibodies recovery and purification from human serum, after contact with [Si][C_3mim]Cl (results in the aqueous medium), [Si][N_{3444}]Cl and [Si][N_{3888}]Cl (results in the materials), using a S:L ratio of 100 mg·mL^{-1}, three different pH values (pH 10, 11 and 12), and a contact time of 60 min.

	[IgG] ± σ (mg·L^{-1})	%Yield$_{IgG}$ ± σ	%Purity$_{IgG}$ ± σ	%Aggregation$_{IgG}$
[Si][C_3mim]Cl				
pH 10	252.3 ± 1.3	85.5 ± 0.4	40.7 ± 0.3	15.2 ± 1.7
pH 11	217.2 ± 0.3	74.0 ± 0.1	52.3 ± 0.7	0.0 ± 0.0
pH 12	77.2 ± 0.8	54.5 ± 0.5	53.1 ± 2.8	0.0 ± 0.0
[Si][N_{3444}]Cl				
pH 10	151.0 ± 40.1	48.8 ± 3.6	70.8 ± 3.3	16.1 ± 2.1
pH 11	144.0 ± 8.2	51.0 ± 2.8	88.9 ± 5.5	15.7 ± 3.0
pH 12	210.0 ± 1.3	23.6 ± 0.5	59.3 ± 0.1	35.3 ± 3.4
[Si][N_{3888}]Cl				
pH 10	129.0 ± 53.2	56.3 ± 8.0	75.4 ± 7.4	16.2 ± 0.2
pH 11	71.9 ± 1.7	75.5 ± 0.6	100 ± 3.3	15.9 ± 6.1
pH 12	222.4 ± 2.3	19.1 ± 0.8	43.1 ± 0.5	31.3 ± 0.9

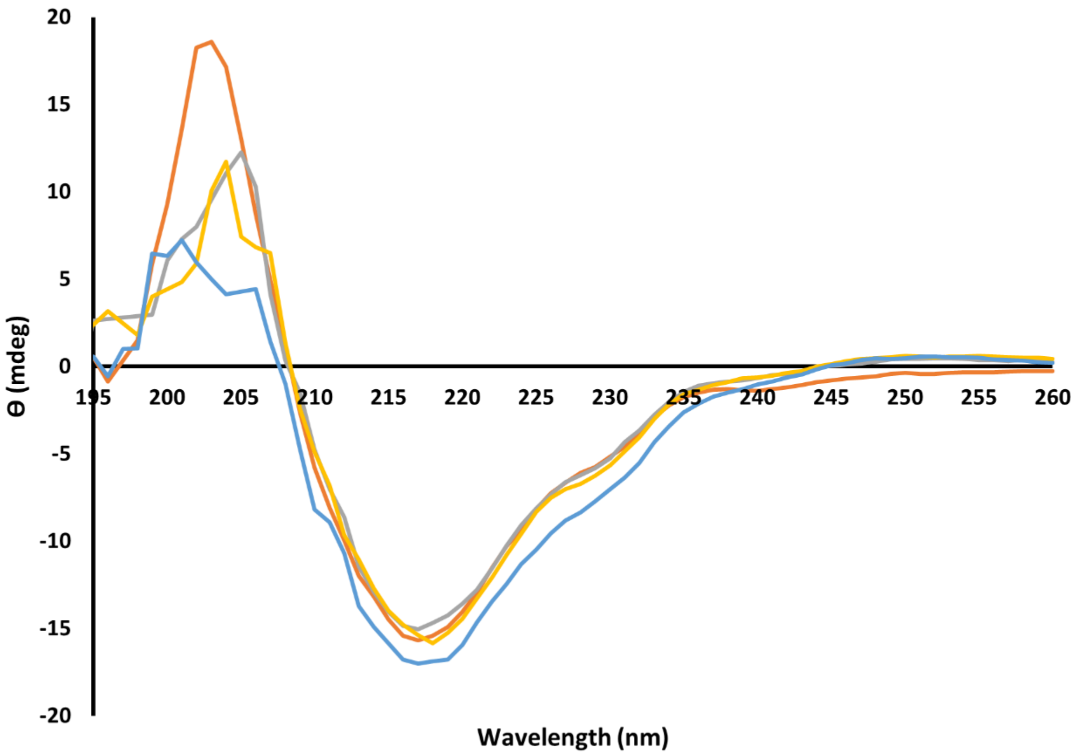

Fig. S14. Circular dichroism spectra of IgG at 25 °C of IgG standard (0.47 mg mL^{-1}) at different pH: 7.4 in PBS (orange), 10 in bicarbonate buffer (grey), 11 in bicarbonate buffer (dark yellow) and 12 in glycine-NaOH buffer (light blue).

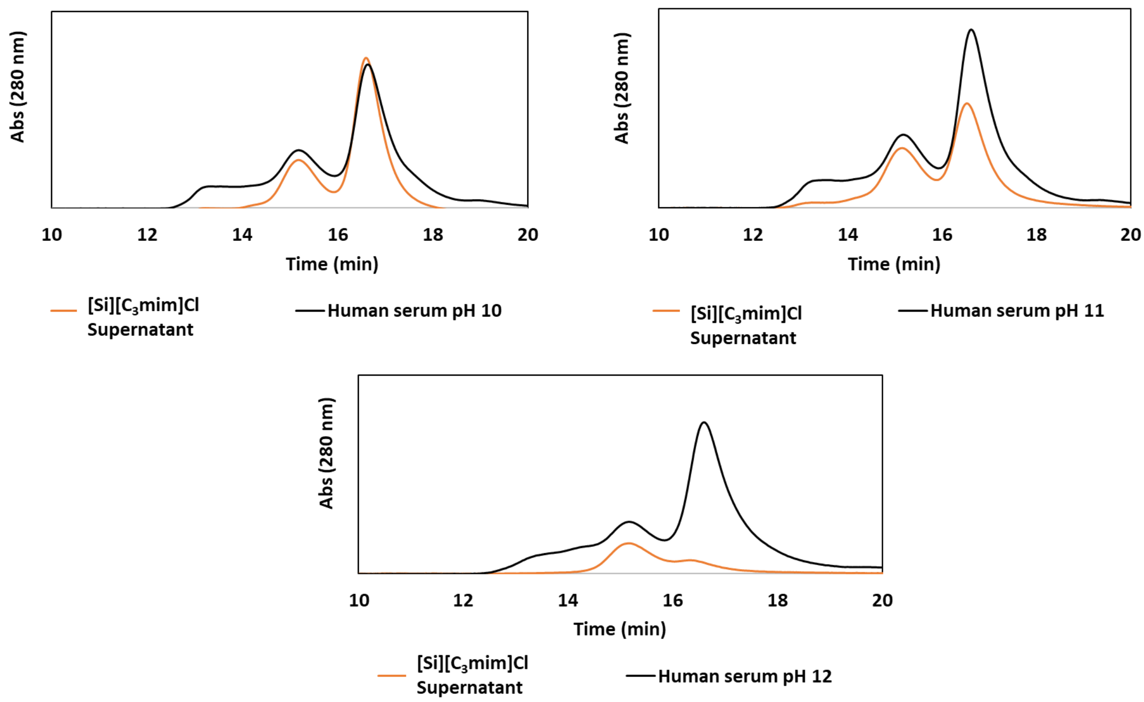

Fig. S15. SE-HPLC chromatograms regarding IgG antibodies recovery and purification from human serum before (—) and after (—) contact with [Si][C_3mim]Cl (supernatant results) with a S:L ratio of 100 mg.mL^{-1} of [Si][C_3mim]Cl and a contact time of 60 min at pH 10, pH 11 and pH12.

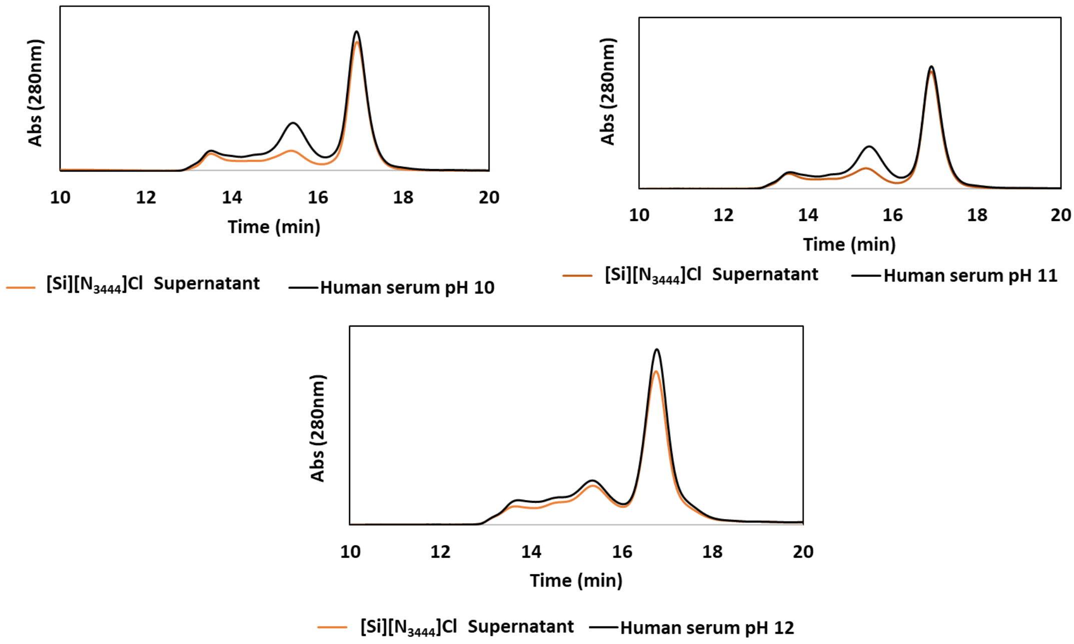

Fig. S16. SE-HPLC chromatograms regarding IgG antibodies recovery and purification from human serum before (—) and after (—) contact with [Si][N_{3444}]Cl (supernatant results), with a S:L ratio of 100 mg.mL^{-1} of [Si][N_{3444}]Cl and a contact time of 60 min at pH 10, pH 11 and pH 12.

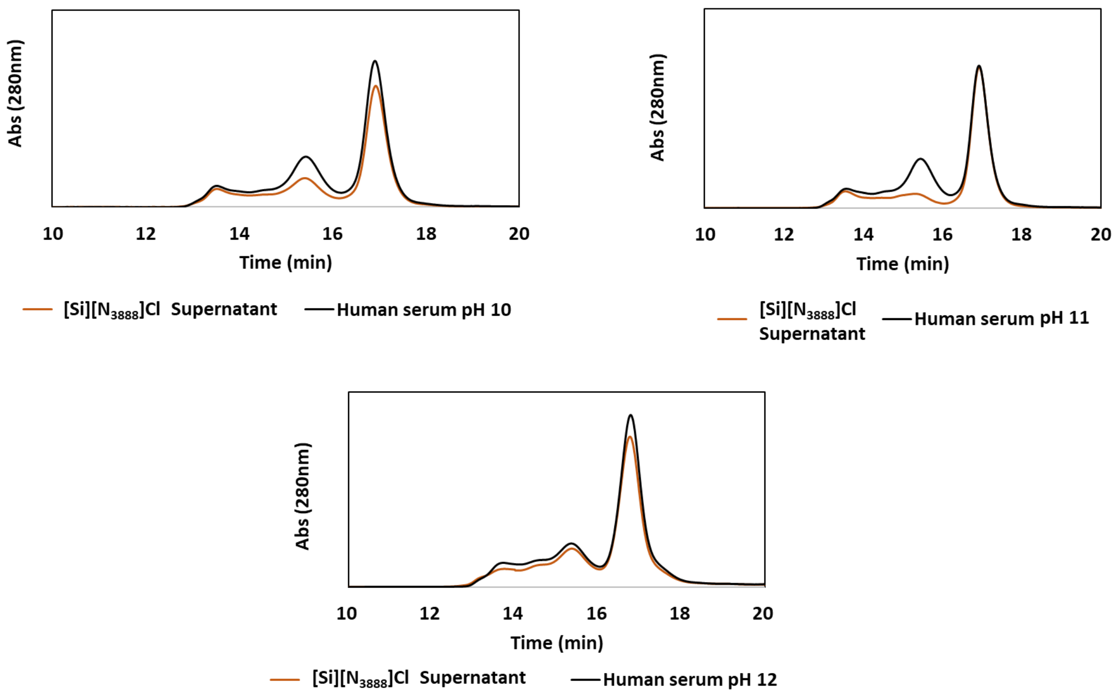

Fig. S17. SE-HPLC chromatograms regarding IgG antibodies recovery and purification from human serum before (—) and after (—) contact with [Si][N_{3888}]Cl (supernatant results), with a S:L ratio of 100 mg.mL^{-1} of [Si][N_{3888}]Cl and a contact time of 60 min at pH 10, pH 11 and pH 12.

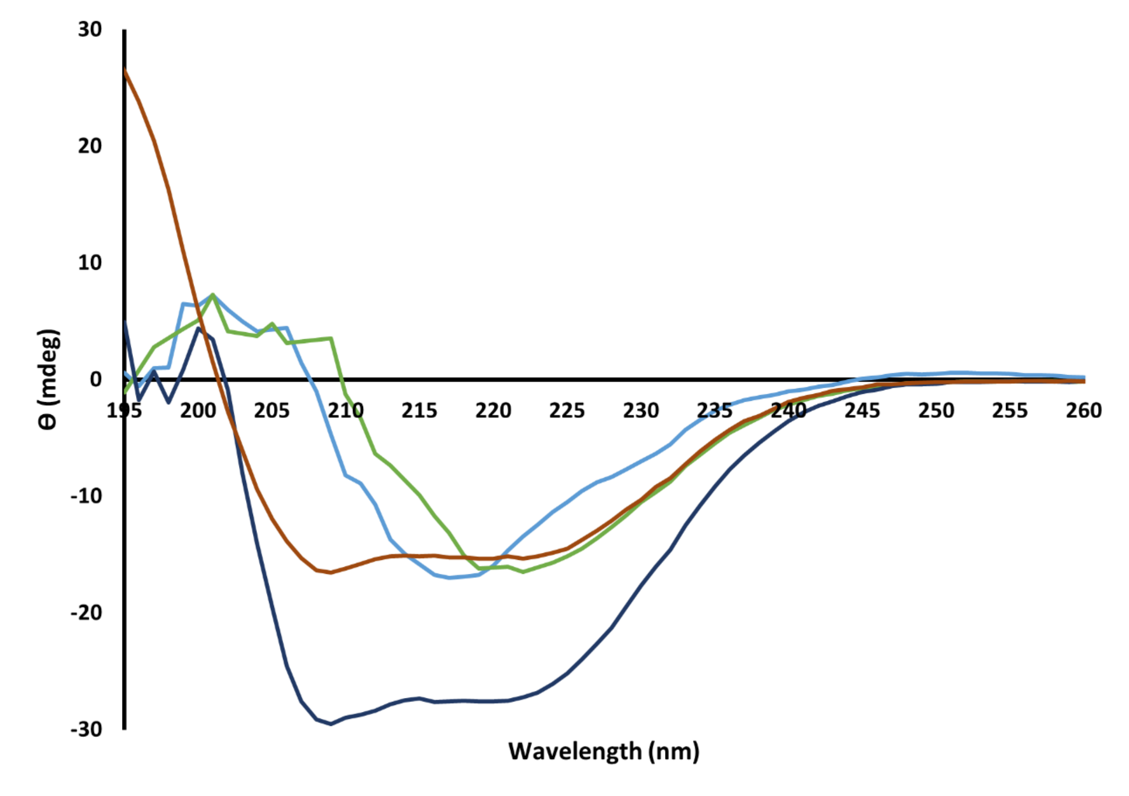

Fig. S18. Circular dichroism spectra of IgG at 25 °C of IgG standard (0.47 mg mL^{-1}) at pH 12 in glycine-NaOH buffer (light blue), HSA standard (0.1 mg mL^{-1}) (dark red), human serum diluted in glycine-NaOH buffer pH 12 (dark blue), and IgG purified using [Si][C3mim]Cl under the optimized conditions (pH 12, S:L ratio 150 mg mL^{-1}, contact time 60 min) (green).

Table S24. Performance parameters ([IgG], %Yield$_{IgG}$, %Purity$_{IgG}$ and %Aggregation$_{IgG}$) regarding IgG antibodies recovery and purification from human serum, after contact with [Si][C$_3$mim]Cl (results in the aqueous medium), using three different S:L ratios (100 mg·mL^{-1}, 150 mg·mL^{-1} and 200 mg·mL^{-1}) and pH values (pH 10, 11 and 12), and a contact time of 60 min.

	[IgG] ± σ (mg·L^{-1})	%Yield$_{IgG}$ ± σ	%Purity$_{IgG}$ ± σ	%Aggregation$_{IgG}$
		pH 10		
100 mg·mL^{-1}	252.3 ± 1.3	85.5 ± 0.4	40.7 ± 0.3	15.2 ± 1.7
150 mg·mL^{-1}	214.4 ± 12.4	79.3 ± 4.6	31.3 ± 1.0	13.1 ± 0.1
200 mg·mL^{-1}	238.2 ± 11.5	88.1 ± 4.3	32.6 ± 0.5	12.3 ± 0.4
		pH 11		
100 mg·mL^{-1}	217.2 ± 0.3	74.0 ± 0.1	52.3 ± 0.7	0.0 ± 0.0
150 mg·mL^{-1}	191.8 ± 4.2	69.2 ± 1.5	48.6 ± 0.7	5.9 ± 0.1
200 mg·mL^{-1}	206.8 ± 10.0	74.5 ± 3.6	42.6 ± 1.6	0.0 ± 0.0
		pH 12		
100 mg·mL^{-1}	77.2 ± 0.8	54.5 ± 0.5	53.1 ± 2.8	0.0 ± 0.0
150 mg·mL^{-1}	83.8 ± 1.1	59.1 ± 0.8	84.2 ± 0.4	0.0 ± 0.0
200 mg·mL^{-1}	78.3 ± 0.6	55.2 ± 0.4	75.4 ± 0.1	0.0 ± 0.0

	[IgG] ± σ (mg·L^{-1})	%Yield$_{IgG}$ ± σ	%Purity$_{IgG}$ ± σ	%Aggregation$_{IgG}$
		[Si][C$_3$mim]Cl		
Human serum	83.8 ± 1.1	59.1 ± 0.8	84.2 ± 0.4	0.0 ± 0.0
CHO cell supernatant	35.9 ± 0.1	85.8 ± 0.2	36.8 ± 0.1	0.0 ± 0.0
Rabbit serum	213.1 ± 5.5	75.7 ± 1.9	51.4 ± 0.6	0.0 ± 0.0
		[Si][N$_{3888}$]Cl		
Human serum	71.9 ± 1.7	75.5 ± 0.6	100.0 ± 3.3	15.9 ± 6.1
CHO cell supernatant	21.7 ± 0.2	48.1 ± 0.5	64.9 ± 0.2	4.4 ± 0.2
Rabbit serum	157.1 ± 0.7	49.8 ± 0.2	96.4 ± 0.3	3.4 ± 0.5

Table S25. Performance parameters ([IgG], %Yield$_{IgG}$, %Purity$_{IgG}$ and %Aggregation$_{IgG}$) regarding IgG antibodies recovery and purification from different complex biological matrices (human serum, CHO cell culture supernatants and rabbit serum), after contact with [Si][C_3mim]Cl (results in the aqueous medium; operation conditions: S:L ratio of 150 mg·mL^{-1}, pH 12 and 60 min of contact time) and [Si][N_{3888}]Cl (results in the material; S:L ratio of 100 mg·mL^{-1}, pH 11 and 60 min of contact time).

	[IgG] ± σ (mg·L^{-1})	%Yield$_{IgG}$ ± σ	%Purity$_{IgG}$ ± σ	%Aggregation$_{IgG}$
		[Si][C_3mim]Cl		
Human serum	83.8 ± 1.1	59.1 ± 0.8	84.2 ± 0.4	0.0 ± 0.0
CHO cell supernatant	35.9 ± 0.1	85.8 ± 0.2	36.8 ± 0.1	0.0 ± 0.0
Rabbit serum	213.1 ± 5.5	75.7 ± 1.9	51.4 ± 0.6	0.0 ± 0.0
		[Si][N_{3888}]Cl		
Human serum	71.9 ± 1.7	75.5 ± 0.6	100.0 ± 3.3	15.9 ± 6.1
CHO cell supernatant	21.7 ± 0.2	48.1 ± 0.5	64.9 ± 0.2	4.4 ± 0.2
Rabbit serum	157.1 ± 0.7	49.8 ± 0.2	96.4 ± 0.3	3.4 ± 0.5

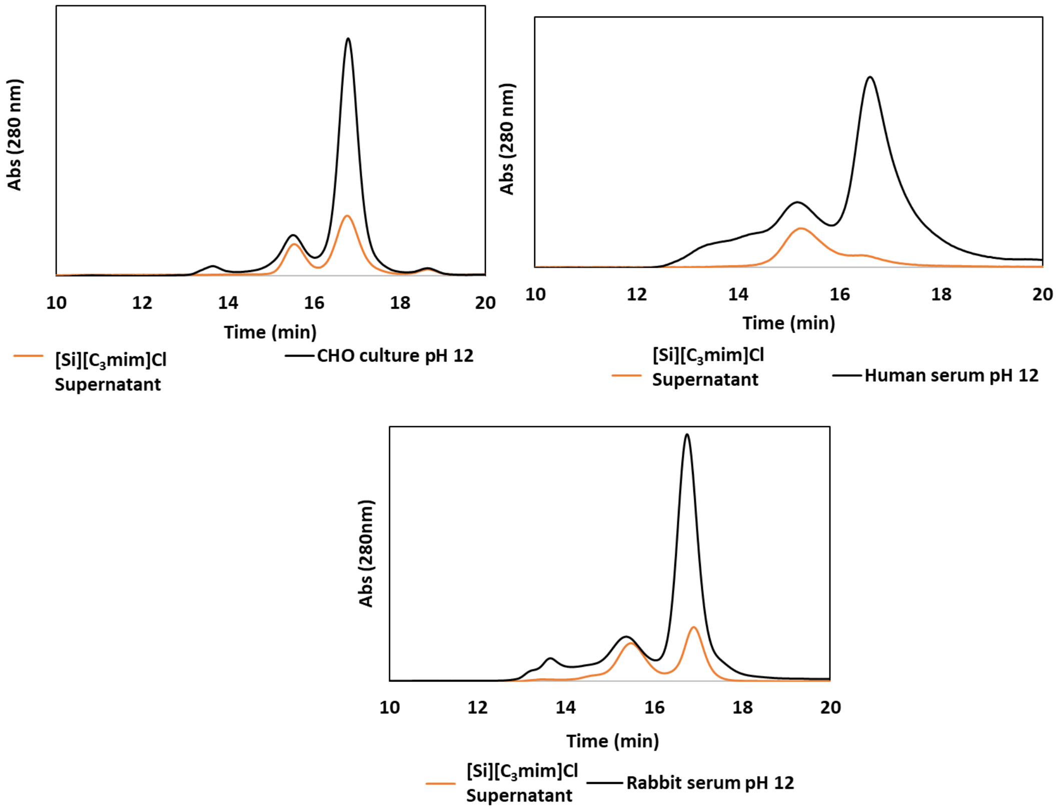

Fig. S19. SE-HPLC cromatrograms for the different complex biological matrices (human serum, CHO cell culture supernatants and rabbit serum), before (—) and after (—) contact with [Si][C_3mim]Cl (Supernatant results; operation conditions: S:L ratio of 150 mg·mL^{-1}, pH 12 and 60 min of contact time).

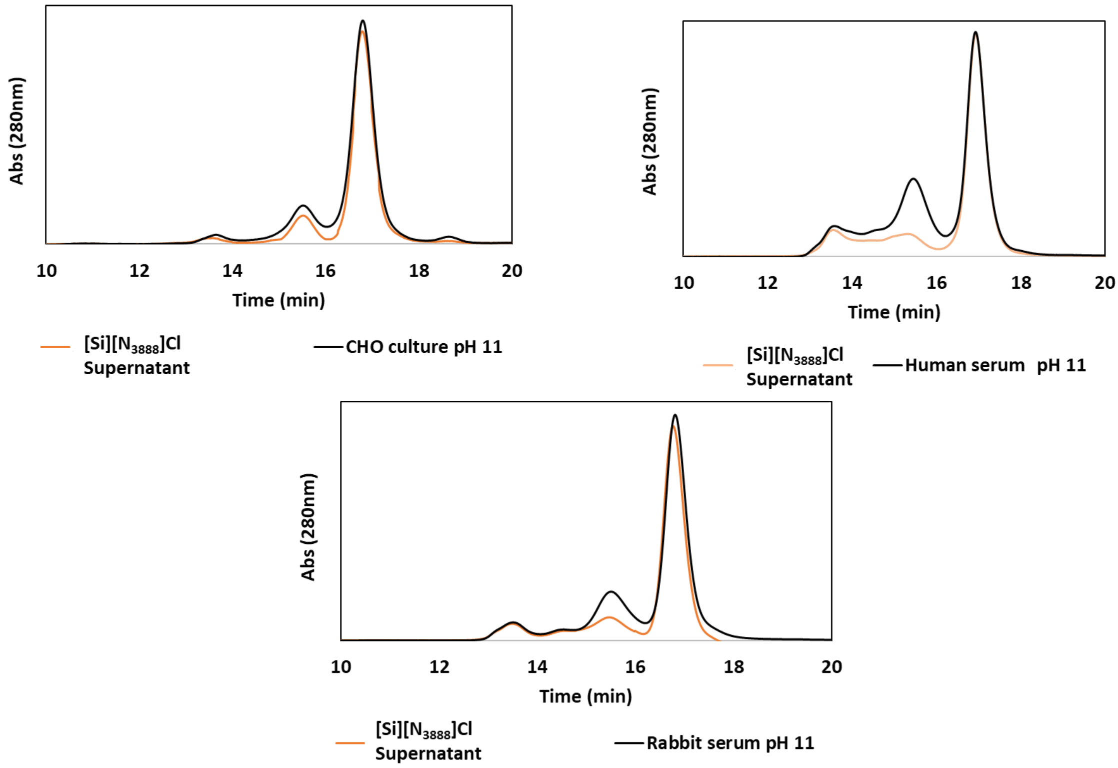

Fig. S20. SE-HPLC chromatograms for the different complex biological matrices (human serum, CHO cell culture supernatants and rabbit serum), before (—) and after (—) contact with [Si][N_{3888}]Cl (Supernatant results; operation conditions: S:L ratio of 100 mg·mL^{-1}, pH 11 and 60 min of contact time).

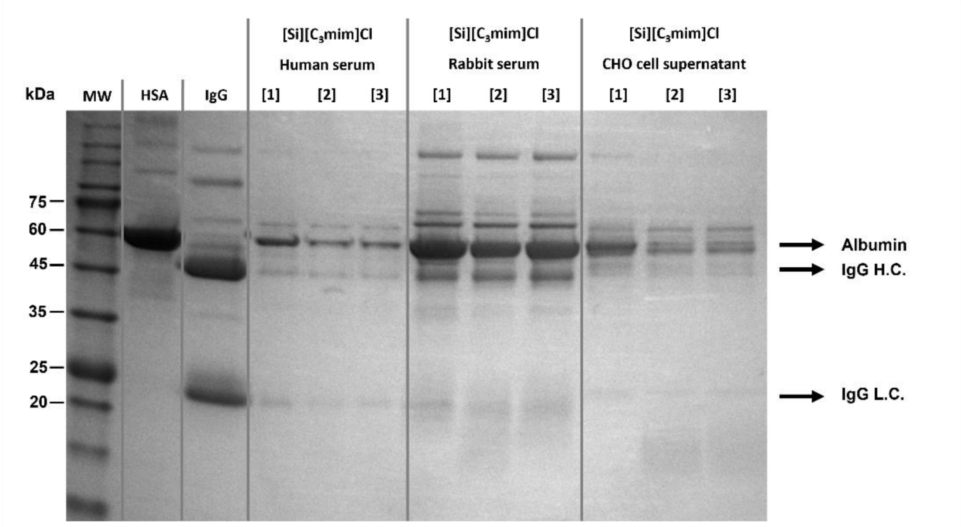

Fig. S21. SDS-PAGE analysis of HSA and IgG standards, and samples purified using [Si][C_3mim]Cl: MW corresponds to the molecular weight marker; for each set of purification experiments, [1] corresponds to the initial IgG-containing sample (20-fold diluted for human and rabbit sera, and undiluted for CHO cell supernatant), and [2] and [3] represent two independent experiments of the flowthrough obtained after purification with [Si][C_3mim]Cl. The bands corresponding to HSA, IgG heavy (H. C.) and light chains (L. C.) are indicated by the arrows.

Table S26. Results from ELISA experiments (Absorbance at 450 and 570 nm) of the different samples and controls (two experiments performed for each condition). The corrected Absorbance (Abs) is obtained by subtracting Abs_{570} to Abs_{450} to correct optical deviations from the plate. A decrease in the corrected Abs in comparison with the negative control – Calibrator diluent RD5P - is indicative of the presence of human anti-IL8 mAbs in the analyzed samples.

Sample	Average Abs_{450}	Average Abs_{570}	Corrected Abs
CHO cell supernatant	2.176	0.062	2.114
CHO cell supernatant pH 12	2.535	0.061	2.474
Flowthrough [Si][C_3mim]Cl	2.815	0.065	2.75
Mouse anti-human CXCL8/IL8	2.299	0.057	2.242
Calibrator diluent RD5P	3.716	0.060	3.656